Optical gas sensing properties of thermally hydrocarbonized porous silicon Bragg reflectors

Tero Jalkanen[1*], Vicente Torres-Costa[2], Jarno Salonen[1], Mikko Björkqvist[1], Ermei Mäkilä[1], Jose Manuel Martínez-Duart[2], and Vesa-Pekka Lehto[1,3]**

[1]*Department of Physics, University of Turku, FI-20014 Turku Finland*

[2]*Departamento de Fisica Aplicada, C-XII, Universidad Autónoma de Madrid, Cantoblanco, 28049 Madrid, Spain*

[3]*Department of Physics, University of Kuopio, P.O.B. 1627, FI-70211 Kuopio Finland*

tero.jalkanen@utu.fi

jarno.salonen@utu.fi

Abstract: In the present work, porous silicon (PS) based Bragg reflectors are fabricated, and the reactive PS surface is passivated by means of thermal carbonization (TC) by acetylene decomposition. The gas sensing properties of the reflectors are studied with different gas compositions and concentrations.

Based on the results it can be concluded that thermally carbonized Bragg reflectors provide an easy and inexpensive means to produce chemically stable high quality PS reflectors with good gas sensing properties, which differ from those of unpassivated PS reflectors.

OCIS codes: (040.6040) Silicon; (230.1480) Bragg reflectors; (280.4788) Optical sensing and sensors; (310.6845) Thin film devices and applications.

References and links

1. L. T. Canham, "Silicon quantum wire array fabrication by electrochemical and chemical dissolution of wafers," Appl. Phys. Lett. **57**, 1046–1048 (1990).
2. L. M. Peter, D. J. Ripley, and R. I. Wielgosz, "In-situ monitoring of internal surface-area during the growth of porous silicon," Appl. Phys. Lett. **66**, 2355–2357 (1995).
3. H. Münder, C. Andrzejak, M. G. Berger, T. Eickhoff, H. Lüth, W. Theiss, U. Rossow, W. Richter, R. Herino, and M. Ligeon, "Optical characterization of porous silicon layers formed on heavily p-doped substrates," Appl. Surf. Sci. **6**, 56–58 (1992).
4. L. T. Canham, "Bioactive silicon structure fabrication through nanoetching techniques," Adv. Mater. **7**, 1033–1037 (1995).
5. R. B. Bjorklund, S. Zangooie, and H. Arwin, "Color changes in thin porous silicon films caused by vapor exposure," Appl. Phys. Lett. **69**, 3001–3003 (1996).
6. V. S.-Y. Lin, K. Motesharei, K.-P. S. Dancil, M. J. Sailor, and M. R. Ghadiri, "A porous silicon-based optical interferometric biosensor," Science **278**, 840–843 (1997).
7. R. C. Anderson, R. S. Muller, and C. W. Tobias, "Investigations of porous silicon for vapor sensing," Sens. Actuators A **21-23**, 835–839 (1990).
8. C. Pickering, M. I. J. Beale, D. J. Robbins, P. J. Pearson, and R. Greef, "Optical properties of porous silicon films," Thin Solid Films **125**, 157–163 (1985).

#106121 - $15.00 USD Received 7 Jan 2009; revised 16 Mar 2009; accepted 17 Mar 2009; published 20 Mar 2009

9. G. Vincent, "Optical properties of porous silicon superlattices," Appl. Phys. Lett. **64**, 2367–2369 (1994).
10. M. G. Berger, C. Dieker, M. Thönissen, L. Vescan, H. Lüth, H. Münder, W. Theiss, M. Wernke, and P. Grosse, "Porosity superlattices: a new class of Si heterostructures," J. Phys. D **27**, 1333–1336 (1994).
11. V. Torres-Costa, R. J. Martín-Palma, and J. M. Martínez-Duart, "Optical characterization of porous silicon films and multilayer filters," Appl. Phys. A **79**, 1919–1923 (2004).
12. P. A. Snow, E. K. Squire, P. St. J. Russell, and L. T. Canham, "Vapor sensing using the optical properties of porous silicon bragg mirrors," J. Appl. Phys. **86**, 1781–1784 (1999).
13. M. S. Salem, M. J. Sailor, F. A. Harraz, T. Sakka, and Y. H. Ogata, "Sensing of chemical vapor using a porous multilayer prepared from lightly doped silicon," Phys. Status Solidi C **4**, 2073–2077 (2007).
14. M. G. Berger, R. Arens-Fischer, M. Thönissen, M. Krüger, S. Billat, H. Lüth, S. Hillbrich, W. Theiss, and P. Grosse, "Dielectric filters made of PS: advanced performance by oxidation and new layer structures," Thin Solid Films **297**, 237–240 (1997).
15. M. Krüger, S. Hilbrich, M. Thönissen, D. Scheyen, W. Theiss, and H. Lüth, "Suppression of ageing effects in porous silicon interference filters," Opt. Commun. **146**, 309–315 (1998).
16. J. Chapron, S. A. Alekseev, V. Lysenko, V. N. Zaitsev, and D. Barbier, "Analysis of interaction between chemical agents and porous Si nanostructures using optical sensing properties of infra-red rugate filters," Sens. Actuators B **120**, 706–711 (2007).
17. M. S. Salem, M. J. Sailor, F. A. Harraz, T. Sakka, and Y. H. Ogata, "Electrochemical stabilization of porous silicon multilayers for sensing various chemical compounds," J. Appl. Phys. **100**, Art. No. 083520 (2006).
18. V. Torres-Costa, J. Salonen, V-P. Lehto, R. J. Martín-Palma, and J. M. Martínez-Duart, "Passivation of nanostructured silicon optical devices by thermal carbonization," Microporous Mesoporous Mater. **111**, 636–638 (2008).
19. V. Torres-Costa, R. J. Martín-Palma, J. M. Martínez-Duart, J. Salonen, and V-P. Lehto, "Effective passivation of porous silicon optical devices by thermal carbonization," J. Appl. Phys. **103**, Art. No. 083124 (2008).
20. J. Salonen, V.-P. Lehto, M. Björkqvist, E. Laine, and L. Niinistö, "Studies of thermally-carbonized porous silicon surfaces," Phys. Status Solidi A **182**, 123–126 (2000).
21. J. Salonen, E. Laine, and L. Niinistö, "Thermal carbonization of porous silicon surface by acetylene," J. Appl. Phys. **91**, 456–461 (2002).
22. J. Salonen, M. Björkqvist, E. Laine, and L. Niinistö, "Stabilization of porous silicon surface by thermal decomposition of acetylene," Appl. Surf. Sci. **225**, 389–394 (2004).
23. M. Björkqvist, J. Salonen, J. Paaski, and E. Laine, "Characterization of thermally carbonized porous silicon humidity sensor," Sens. Actuators A **112**, 244–247 (2004).
24. M. Björkqvist, J. Salonen, E. Laine, and L. Niinistö, "Comparison of stabilizing treatments on porous silicon for sensor applications," Phys. Status Solidi A **197**, 374–377 (2003).
25. CRC Handbook of Chemistry and Physics 88th edition, D. R. Lide, ed., (CRC Press/Taylor and Francis, Boca Raton, FL, 2007-2008).
26. J. McMurry, in: Organic Chemistry (5th edition), (Thomson Brooks/Cole,2000).
27. H. A. Macleod, in: Thin-film optical filters (Second edition), (Adam Hilger Ltd, Bristol, 1986), chap. 5.
28. V. Torres-Costa, J. Salonen, T. Jalkanen, V-P. Lehto, R. J. Martín-Palma, and J. M. Martínez-Duart, "Carbonization of porous silicon optical gas sensors for enhanced stability and sensitivity," Phys. Status Solidi A, **1-3** (2009)/DOI 10.1002/pssa.200881052.

1. Introduction

Properties of PS have been studied extensively since the discovery of visible photoluminescence at room temperature [1]. Interesting material properties, such as a high internal surface area [2], tunable refractive index [3] and biocompatibility [4], make PS a strong candidate for a material to be used in various applications. In particular, the large specific surface area of PS can be utilized in different gas sensing applications. The adsorption of gas molecules into the pores modifies the optical [5, 6] and electrical [7] properties of the substance, and this can be used to detect variations in the ambient gas atmosphere.

PS is usually manufactured from crystalline silicon with an electrochemical etching process conducted in a hydrofluoric (HF) acid based solution. The porosity of the PS layer may be controlled by adjusting the anodization current. From an optical point of view, PS may be considered as a homogenous effective medium. The refractive index of the layer depends mainly on the porosity, and therefore it may also be altered easily by changing the anodization current density [8]. This allows the fabrication of optical interference filters, such as distributed Bragg reflectors and Fabry–Pérot filters, by simply producing stacks of carefully dimensioned PS layers with alternating porosities [9, 10, 11]. The characteristic feature of these multilayer re-

#106121 - $15.00 USD Received 7 Jan 2009; revised 16 Mar 2009; accepted 17 Mar 2009; published 20 Mar 2009

flectors is a distinct reflectance band observed in the reflectance spectra. These regions of high reflectivity, found at certain wavelengths, are due to the constructive interference that takes place in the filter structure. Moreover, infiltration of chemical species to the porous structure affects the optical properties of the effective medium. Consequently, PS interference reflectors may be used for optical gas sensing by measuring the redshift, which may be observed in the reflectance spectra, when the reflectors are exposed to different chemical vapours [12, 13].

The natural oxidation that takes place in as-anodized PS layers has been the biggest obstacle in developing practical gas sensing applications utilizing PS optical filters. This so called ageing, i.e. progressive oxidation of the porous structure, leads to gradual blue shift of the reflectance spectrum and may also impair the overall optical performance of the multilayer structure. Therefore, chemical stability is an important issue, especially in applications where the reflectors are required to recover from multiple adsorption desorption cycles. Stabilization of PS multilayer structures by means of different oxidation processes, such as thermal [14, 15], chemical [15, 16] and electrochemical oxidation [17], has been reported previously. However, oxidation leads to a dramatic reduction of the specific surface area of the porous structure, thereby decreasing its sensitivity for ambient adsorbates. In addition, the refractive index of silicon oxide is lower than that of silicon, and this may have undesired effects on the optical performance of the filter. Recent studies have shown that effective stabilization of PS based optical structures can also be achieved by thermally carbonizing the porous structure by means of acetylene decomposition [18, 19]. Thermal carbonization provides effective passivation of the PS structure and preserves the majority of the specific surface area [20]. It also provides the option of affecting the surface chemistry in a way that either hydrophobic or hydrophilic surface may be achieved, simply by adjusting the treatment temperature [21].

In the present study, the gas sensing properties of thermally hydrocarbonized PS Bragg reflectors were investigated. For that purpose, PS reflectors were exposed to different gas mixtures, and their reflectance spectra were measured as a function of atmospheric composition. Furthermore, response time measurements were performed in order to study the responsiveness of the devices.

2. Experimental

2.1. Fabrication of the Bragg reflectors

The samples were prepared by electrochemical etching of a boron doped p^+-type silicon substrate, with resistivity of $0.01 - 0.02\,\Omega$cm and $\langle 100 \rangle$ crystal orientation. The electrolyte used for the etching consisted of a 1:1 mixture of absolute ethanol and hydrofluoric (HF) acid (38 wt %). The production of Bragg reflectors was conducted by controlling the anodization current density, while other etching parameters were kept constant. The current density was modulated discretely between 10 and 100 mAcm^{-2}, so that a Bragg reflector design consisting of 10 bilayers was reached. Proper etching times were calculated by determining the formation rate of the optical layer thickness for the particular current densities. The etching times were 13.0 and 3.94 s, respectively. One etch cycle was comprised of etching two consecutive layers followed by an etch stop of 1 s, which was intended to level out possible concentration gradients in the electrolyte solution inside the pores. The anodization current was supplied by a computer controlled Agilent Technologies N5749A DC power supply, which enabled accurate control over current density and etching time.

The optical thickness formation rate was derived from optical thicknesses of PS single layers produced with varying etch times. Reflectance measurements were used to calculate the optical thicknesses, i.e. the product of the layer thickness and the refractive index of the porous material, for individual layers. Based on these calculations, the etch times for Bragg reflector

#106121 - $15.00 USD Received 7 Jan 2009; revised 16 Mar 2009; accepted 17 Mar 2009; published 20 Mar 2009

production were determined so that each layer fulfilled the Bragg condition:

$$nd = \frac{\lambda_0}{4}, \tag{1}$$

where n is the refractive index, d is the layer thickness and λ_0 is the resonant wavelength. The optical layer thicknesses were adjusted in a way which resulted to stopband formation in the infrared range. The resonant wavelength of the reflectors was located in the proximity of 1400 nm. Obtained reflectance spectrum for one of the Bragg reflectors fabricated is shown in Fig. 1.

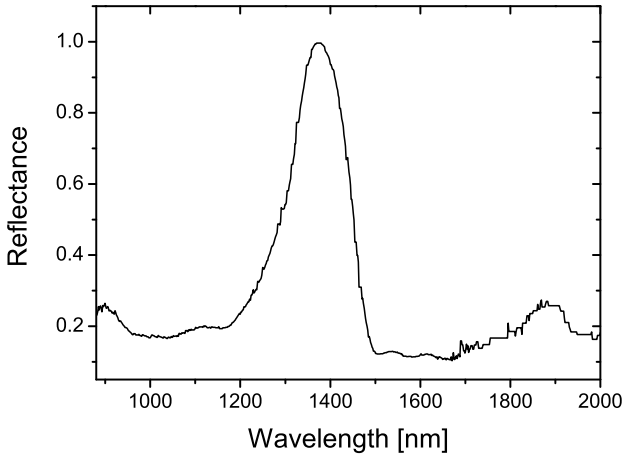

Fig. 1. The measured reflectance spectrum for a thermally hydrocarbonized Bragg reflector.

2.2. Thermal carbonization

After anodization, the samples were rinsed in absolute ethanol and then dried at room temperature for approximately 2 hours. The dried samples were placed in a sealed quartz-tube and kept under constant nitrogen flow for 30 min. The treatment was continued by introducing an acetylene flow to the tube, and a continuous flow of acetylene and nitrogen in 1:1 volumetric fraction was continued for 10 min. Finally the samples were placed in a furnace and kept at 500 ºC for 10 min in a constant flow of acetylene and nitrogen. After the heat treatment the samples were cooled down under constant N_2 flow until they reached room temperature.

Temperatures below 600 ºC enable the use of continuous acetylene flush during the treatment without problems arising from the graphitization of acetylene. Carbonization in this temperature regime also leads to a hydrophobic surface [22]. Hydrophilic surfaces may be obtained by increasing the temperature used for the heat treatment above 680 ºC [22]. Therefore, surfaces treated in higher temperatures can be used for humidity sensing applications [23]. In general, thermal carbonization has been found as an attractive stabilization method for PS sensor applications [24].

2.3. Experimental setup

The thermally hydrocarbonized (THC) samples were placed in a measurement chamber, into which nitrogen flow was introduced through a gas line. Vapours of varying chemical species were introduced to the chamber by bubbling a fraction of the nitrogen carrier flow through a liquid phase of the species studied. The total amount of nitrogen flow was kept constant at

#106121 - $15.00 USD Received 7 Jan 2009; revised 16 Mar 2009; accepted 17 Mar 2009; published 20 Mar 2009

250 ml/min, and the concentration of the studied chemical species was changed by modifying the amount of nitrogen led to the bubbling chamber. Fourier transform infrared spectroscopy (FTIR) measurements were performed with a Perkin Elmer Spectrum BX FTIR spectrometer, in order to determine the gas concentrations for different bubbling fractions of the chemical species studied. The studied chemical compounds and their concentrations are presented in Table 1.

Reflectance measurements were carried out in the infrared range with wavelengths extending from 880 nm to 2000 nm. The electromagnetic radiation was created with a 100 W Xenon short arc lamp, and a monochromator was used for controlling the wavelength. The infrared radiation was led to the measurement chamber via optical fibre, and the reflected light intensity was measured with an InGaAs-photodetector.

Table 1. Volumetric vapour concentrations obtained with different gas flow ratios. Gas flow ratio indicates the fraction of the nitrogen carrier flow led to the bubbling chamber.

Gas flow ratio	0.2	0.4	0.6	0.8
Acetone	2.85 %	8.38 %	11.4 %	12.7 %
Decane	0.015 %	0.044 %	0.068 %	0.088 %
DMF	0.003 %	0.011 %	0.049 %	0.063 %
Hexane	2.99 %	6.17 %	8.64 %	10.1 %
Methylamine	3.84 %	8.05 %	11.5 %	13.7 %
Toluene	0.047 %	0.052 %	0.805 %	1.33 %

3. Results and Discussion

3.1. Effects of the atmospheric composition

A clear redshift in the reflectance spectra was observed for all the gases studied. Moreover, the value of the redshift increased as a function of the vapour concentration. This can be seen clearly from Fig. 2, which presents the obtained redshifts for different gas flow ratios. When the redshifts are examined as a function of vapour concentration, a linear dependence between the vapour induced redshift and the adsorbate concentration can be noted. An exception to this trend is observed for hexane atmosphere, where the redshift seems to grow as an exponential-like function of the concentration. However, since the dispersion in the measured reflectance band redshift values, obtained for larger concentrations of hexane, is quite notable, definite conclusions regarding its behaviour can not be made. Minor divergence from linear growth may also be observed for smaller concentrations of decane, dimethylformamide (DMF), and toluene, but these differences are most likely caused by small variations of the adsorbate vapour pressure. The effects of hexane vapour exposure are presented in Fig. 3.

In addition to the spectral redshift, it became obvious that the overall shape of the spectra was also slightly altered when the reflectors were subjected to the studied vapours. This effect is easy to understand, because the adsorbate gas modifies the optical properties of the effective medium matrix. Even though the qualitative verification of this phenomenon is easily obtained, a quantitative analysis method that would allow a simple, yet reliable method for spectral shape alteration comparison, is difficult to develop. In order to monitor the spectral alterations, the full width at half maximum (FWHM) values of the reflectance spectra stopbands were measured. From the measured FWHM values, it can be concluded that acetone, decane and methylamine have the strongest effects on the shape of the spectrum. DMF, hexane and toluene also affected the observed shape, but in most cases their influence was negligible. A clear increase in the FWHM value was observed for acetone vapour. For higher concentrations, the increase was as

#106121 - $15.00 USD Received 7 Jan 2009; revised 16 Mar 2009; accepted 17 Mar 2009; published 20 Mar 2009

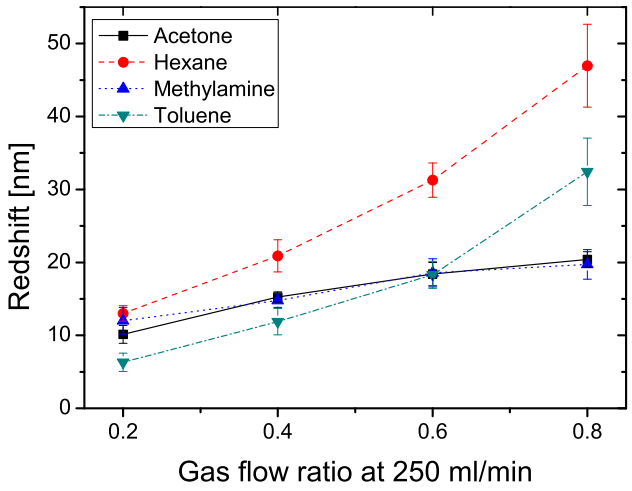

Fig. 2. The measured redshifts for different flow ratios. The redshifts presented are the mean values of three measurements. Standard deviation for the data points is also included in the graph.

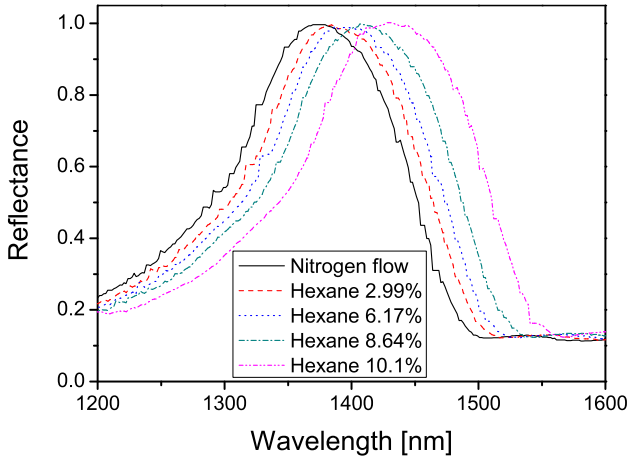

Fig. 3. Redshift induced by hexane vapour adsorption to the porous structure.

large as 10 nm, which is almost 7 % of the initial FWHM value of the stopband, measured in pure nitrogen flow. It is normal that the stopband FWHM value increases when the specrum shifts to larger wavelengths, but for acetone the observed increase was too large to be explained by this phenomenon. Contrary to acetone, decane caused a 9 % decrease in the observed FWHM value. It is also noteworthy that the decane concentrations were extremely low, when compared to those of acetone. Figure 4 shows the measured FWHM values as a function of gas flow ratio for acetone, decane, and methylamine.

Vapour induced spectral alterations may provide means to obtain selectivity for optical sensors, as presented in Fig. 5. It can be seen from Fig. 5(a), that there is no notable difference in the observed redshift of the reflectance spectra stopband, when the reflector is subjected to acetone and methylamine vapours. However, when we look at the stopband alteration, it can be noted that acetone causes an increase in the FWHM value, whereas a decrease is observed for

#106121 - $15.00 USD Received 7 Jan 2009; revised 16 Mar 2009; accepted 17 Mar 2009; published 20 Mar 2009

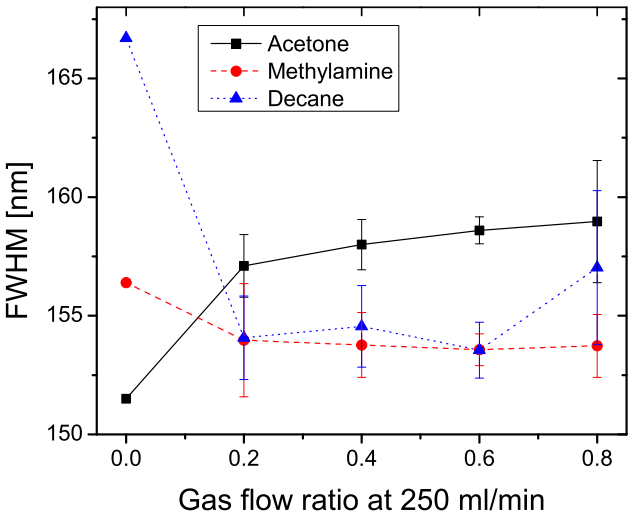

Fig. 4. Full width at half maximum values as a function of gas flow ratio for acetone, decane, and methylamine.

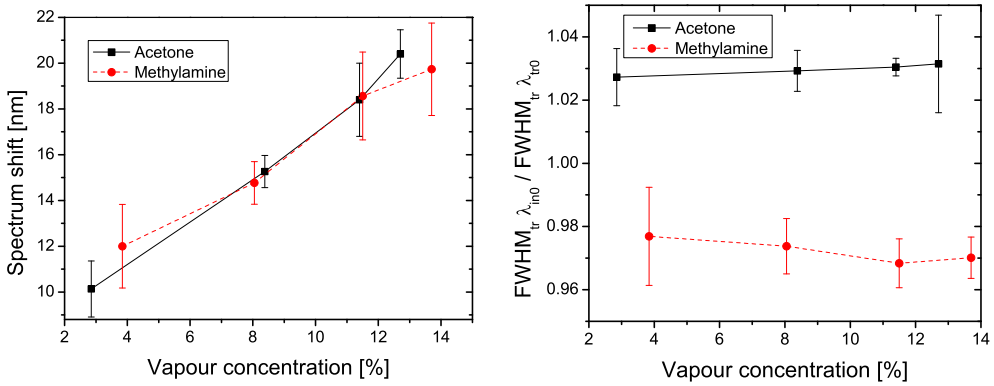

(a) The spectral redshifts measured under acetone and methylamine vapour exposure.

(b) Relative change of the normalized FWHM value as a function of acetone and methylamine vapour concentration.

Fig. 5. The acetone and methylamine induced spectral redshifts of the resonant wavelength are almost identical, as shown in graph a). However, the influence that the adsorbants have on the shape of the observed spectrum is totally different. Acetone widens the stopband, whereas methylamine has the opposite effect. This behaviour can be seen for the FWHM values recorded for the reflective stopbands, which are presented in graph b).

methylamine. This is illustrated in Fig. 5(b), in which the ratio between the normalized value of the transformed FWHM ($FWHM_{tr}$) and the normalized initial FWHM ($FWHM_{in}$) value is shown for different concentrations. The ratio is described by the expression:

$$\frac{\mathrm{FWHM_{tr}}/\lambda_{tr0}}{\mathrm{FWHM_{in}}/\lambda_{in0}} = \frac{\mathrm{FWHM_{tr}}\lambda_{in0}}{\mathrm{FWHM_{in}}\lambda_{tr0}}, \tag{2}$$

where λ_{tr0} is the resonant wavelength for the shifted spectra and λ_{in0} is the resonant wavelength of the initial reference spetrum. Normalized FWHM values were used here to rule out the

#106121 - $15.00 USD Received 7 Jan 2009; revised 16 Mar 2009; accepted 17 Mar 2009; published 20 Mar 2009

influence of the stopband growth caused by the spectral shift to larger wavelengths.

It is reasonable to assume that several properties of the adsorbate gas affect the detected reflectance spectrum. The refractive index, dielectric constant, and saturated vapour pressure values for the studied vapours are presented in Table 2. Although the refractive index and the dielectric constant are in close relation to each other, the static dielectric constant evaluated for a frequency of zero is a better measure for permanent electric dipole moments than the refractive index. It can be seen that acetone, DMF, and methylamine have relatively large dielectric constant values, when compared to decane, hexane, and toluene, and more importantly that the values do not correlate with the refractive index values. Large dielectric constant values would provide a logical explanation for the alterations observed in the reflectance spectra stopband width, since dielectric constant, or more precisely the dielectric function, describes the interaction between the incident electromagnetic wave and the adsorbent-adsorbate system. However, as it was previously stated, DMF, which has the largest dielectric constant value, does not exhibit notable changes in the FWHM value of the stopband. Conversely, decane which has a fairly low dielectric constant value causes a substantial decrease to the observed FWHM value. Therefore, it is rather obvious that the differences observed in the stopband width are not directly related to the dielectric constant value of the adsorbate gas molecules.

Table 2. Refractive indices n, dielectric constant values ε, and the saturated vapour pressure values p_0 for the studied substances [25, 26]. *The p_0 value for methylamine is for a solution consisting of 60% water and 40% methylamine.

Chemical species	n	ε	p_0 [mbar]
Acetone	1.359	20.49	246.0
Decane	1.409	1.985	1.900
Dimethylformamide	1.431	38.25	3.600
Hexane	1.375	1.882	165.3
Methylamine	1.351	12.65	646.6*
Toluene	1.497	2.374	38.00

Alternative explanation for the changes in the FWHM values of the reflectance spectra may be found from the adsorption behaviour of the adsorbate gas molecules. The width of the reflectance spectrum stopband is related to the refractive index difference of the high and low index layers [27]:

$$\frac{\Delta\lambda}{\lambda_0} = \frac{4}{\pi}\arcsin\left(\frac{n_H - n_L}{n_H + n_L}\right). \tag{3}$$

The high index layers of PS Bragg reflectors result from a lower etching current density. Small current density also produces pores with a smaller pore radius. Therefore, some adsorbate molecules might have a higher affinity to one of the layer types, which would explain the observed changes in the stopband width. For example, the large decrease in the stopband width caused by decane, might be explained by a higher affinity to the small refractive index layers. The behaviour observed for acetone and methylamine, shown in Fig. 5, can be explained by assuming that they produce the same change in the overall effective refractive index n, but affect the high porosity (n_L) and low porosity (n_H) layers differently.

The effect of the adsorbate refractive index was also considered, but no direct correlation between the refractive index and observed redshift of the reflectance spectra was found. However, the vapour induced redshift seems to be connected to the saturated vapour pressure value (p_0) of the adsorbate molecules. This is presented in Fig. 6. It can be seen that there is a correlation between the relative redshift and p_0 values of the studied vapours. The relative redshift value is

#106121 - $15.00 USD Received 7 Jan 2009; revised 16 Mar 2009; accepted 17 Mar 2009; published 20 Mar 2009

basically the redshift gradient, which was obtained by differentiating the redshift in respect to the vapour concentration. Based on Fig. 6, it can be concluded that gasses that possess a small p_0 value produce a larger relative redshift. This in turn will give a better sensitivity for those kinds of gasses.

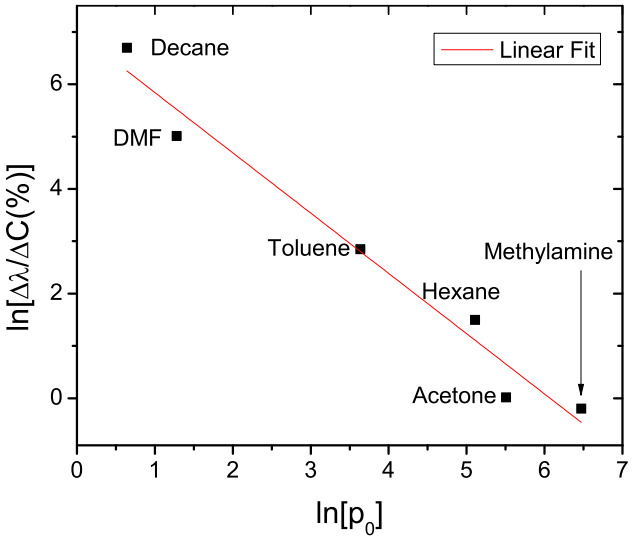

Fig. 6. A correlation between the relative redshift and the saturated vapour pressure values was observed. Low value of the saturated vapour pressure leads to a higher sensitivity for the gas molecules.

3.2. Response time measurements

Response time measurements were carried out by monitoring the reflected light intensity at a fixed wavelength. The wavelength was set at 1520 nm. This wavelength was chosen, because the right-hand side of the stopband is located in this region. Therefore, redshifts related to the gas adsorption will cause a rise in the photodiode output voltage. This behaviour is demonstrated for methylamine in Fig. 7.

The time-resolved measurement, presented in Fig. 7, shows that the reflector gives an immediate response, when methylamine vapour is introduced to the measurement chamber at t = 20 s. It can also be seen that the output voltage of the photodiode increases in co-ordinance with increasing concentration, as expected. However, for higher concentrations, the voltage signal does not level out during a 3 min exposure time. This phenomenon is most likely related to the adsorption properties of methylamine. Similar measurements performed for acetone and hexane vapours are presented in Fig. 8. The reflector response is even faster for acetone and hexane, and the voltage signal level seems to balance out well. It is also noteworthy that the recovery time after vapour exposure is fast, and the signal returns to its original value, even after several cycles of adsorption and desorption. The response and recovery times for decane, DMF, and toluene vapours were also found fast.

Reflector response is closely related to the adsorption properties of the studied vapour. Adsorption process, is determined by the properties of the adsorbate and the adsorbent. Therefore, the observed response time is not the same for different vapours. For example, the polarity of the adsorbate may influence its probability to stick to a certain surface. Adjusting the pore size, should allow the fabrication of a surface that is more attractive to certain molecules, making

#106121 - $15.00 USD Received 7 Jan 2009; revised 16 Mar 2009; accepted 17 Mar 2009; published 20 Mar 2009

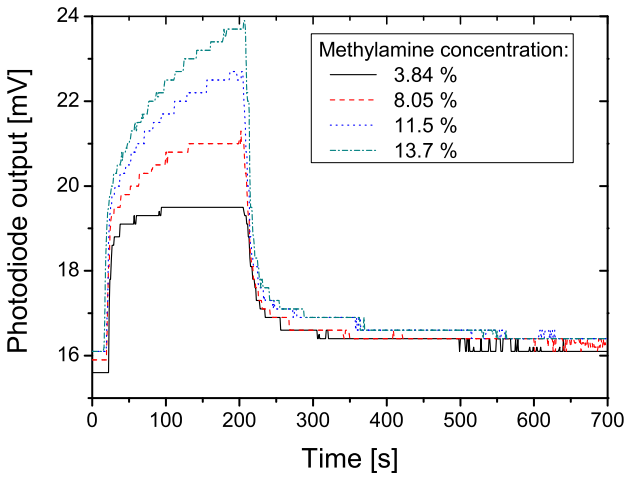

Fig. 7. Time-resolved photodiode response measurement for methylamine vapour at a fixed wavelength of 1520 nm.

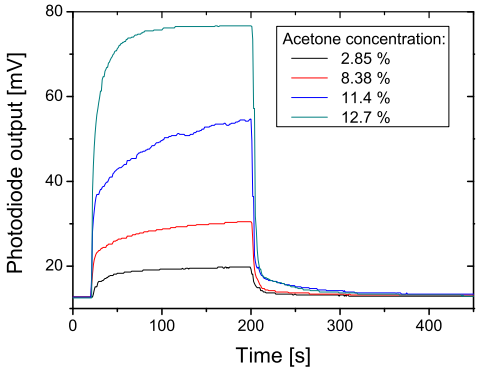

(a) Photodiode output voltage with varying acetone vapour concentrations.

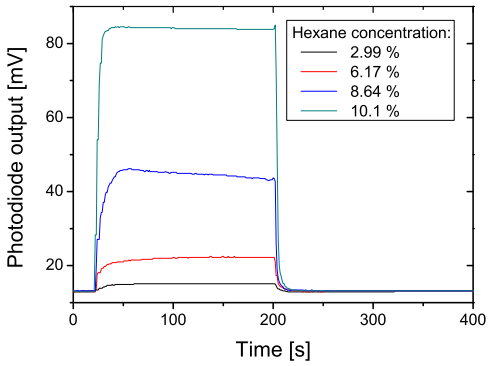

(b) Photodiode output voltage with varying hexane vapour concentrations.

Fig. 8. Time-resolved measurement that describes the reflected light intensity at λ = 1520 nm. Acetone and hexane were introduced in the measurement chamber with a nitrogen carrier flow at $t = 20$ s and flushed away at $t = 200$ s.

the reflector response faster. However, in the case of optical reflectors, the optical parameters for individual layers also require careful consideration. Therefore, fine-tunement of the etching parameters for enhancing the adsorption of certain gases might be a long and tedious process with little practical relevance.

3.3. Effects of thermal carbonization

It has been reported that the effects of thermal carbonization (TC) on the optical properties of the reflector are quite small [28]. For example, the changes that the PS surface passivation has on the resonant wavelength are much smaller than, e.g. electrochemical oxidation [17]. In some cases, TC treatment may even be used to increase the sensivity of the optical sensor [28].

As it was pointed out, the response times for thermally hydrocarbonized (THC) Bragg reflectors were fast. Hence, it can be concluded that the THC surface treatment seems to be suitable

#106121 - $15.00 USD Received 7 Jan 2009; revised 16 Mar 2009; accepted 17 Mar 2009; published 20 Mar 2009

for practical applications. Time-resolved measurements also revealed that the redshift caused by vapour adsorption is a fully reversible process. This indicates that the surface treatment has succesfully stabilized the structure.

The hydrophobicity of the hydrocarbonized sensor was also tested by exposing it to humidity. There was no notable change in the reflectance spectra observed for humidity values up to 50 RH%. This demonstrates that the redshift observed for different chemical vapours was not caused by humidity.

4. Conclusions

Based on the presented results, we can conclude that thermally hydrocarbonized PS Bragg reflectors possess good gas sensing properties. The redshift values obtained from the reflectance spectra, were shown to increase as a function of the vapour concentration. It was also shown that spectral shape alterations may provide some level of selectivity in gas sensing. The effect of humidity as a cause of the redshift was also ruled out by using the hydrophobic hydrocarbonized silicon surface. This enables the use of the reflectors for specific gas sensing purposes even in humid environments.

Time-resolved measurements revealed that the sensors produce a rapid response, when the atmospheric composition is changed. Recovery time after vapour exposure was also found to be fairly fast. Moreover, it was discovered that the sensors can fully recover from multiple cycles of adsorption and desorption. This quality is of the utmost importance when practical applications are considered. It basically demonstrates the prolonged usability of the sensors, which is a requirement for gas sensing applications.

Acknowledgments

This work was supported by Academy of Finland (grant no. 109226).

#106121 - $15.00 USD Received 7 Jan 2009; revised 16 Mar 2009; accepted 17 Mar 2009; published 20 Mar 2009